The Effect of a 'Smart' Predator in a One Predator, Two Prey System*

Elizabeth Green

October 16, 2004

Abstract

This paper analyzes a food web with a predator and two non-competing preys where the predation follows the density gradient of the prey. The long-term dynamics of the food web and short-term population crashes and outbreaks are analyzed using singular perturbation analysis.

1 Introduction

A model for an ecological system of one predator and two preys is considered in this paper. There is no competition between the preys. The predator divides its time between the two preys and the time it spends hunting for each prey depends on the comparative density of the preys. This paper focuses on analyzing the populations for various parameter values in the model using nullcline analysis, singular perturbation analysis, and numerical experimentation. More specifically, it focuses on new phenomena not seen in similar models that do not assume the prey density dependent predation. One such phenomenon is the existence of a stable equilibrium when the predator is efficient with respect to both preys. This is surprising. In the classical theory of one predator and one prey, an efficient predator always results in a stable limit cycle and the addition of another prey (without density dependent predation) also leads to cycles [1]. Another interesting phenomenom is the existence of chaotic dynamics due to Shilnikov orbit. This paper aims to show that in modeling an ecosystem the type of predation is important and the dynamics become richer with more realistic assumptions.

*Faculty advisor was Dr. Bo Deng and this work was funded by the UCARE Program.

2 Deriving the Model

The preys are assumed to grow logistically in the absence of the predator. If $X(t)$ is the number of a prey and there are no predators, then the logistic model gives $\frac{dX}{dt} = rX(1 - X/K)$, where r is the birth rate and K is the carrying capacity (the maximum population that the environment can theoretically sustain). If $Z(t)$ is the number of predators, then assuming that the predator dies off exponentially in the absence of prey gives $\frac{dZ}{dt} = -dZ$.

Understanding the effects of predation involve determining by what amount predation decreases the growth rate of the prey and increases the growth rate of the predator. In his seminal paper, C. S. Holling, in 1959, devised an experiment from which he obtained what is now known as the Holling Type-II disc function on a single prey [5]. For this two-prey system, Holling Type-II predation is modified in the following way. Assume that prey one and prey two cannot be hunted simultaneously and in a given time T, the predator Z spends $T_1 = \frac{X}{X+cY}T$ time on prey one, X, and $T_2 = \frac{cY}{X+cY}T$ on prey two, Y. The parameter c represents the desirability of prey Y relative to prey X. Notice that if X and Y are comparable, then $c \to 0$ means that all time is spent on prey X while $c \to \infty$ means that all time is spent on prey Y. Let T_{H_i} be the handling time of each prey. The handling time represents the time it takes the predator to eat and digest the prey. Let a_i be the predator's probability of finding prey, which is assumed to be constant following the usual form of Holling Type-II predation. Let X_T be the amount of prey X caught, and Y_T be the amount of prey Y caught. This leads to the equations:

$$\begin{cases} X_T &= a_1(T_1 - T_{H_1}X_T)X \\ Y_T &= a_2(T_2 - T_{H_2}Y_T)Y. \end{cases}$$

Solving for the predation rates gives:

$$\begin{cases} \dfrac{X_T}{T} &= \dfrac{\frac{X}{X+cY}a_1X}{1 + a_1T_{H_1}X} &= \dfrac{p_1X}{H_1 + X}\dfrac{X}{X + cY} \\ \dfrac{Y_T}{T} &= \dfrac{\frac{cY}{X+cY}a_2Y}{1 + a_2T_{H_2}Y} &= \dfrac{p_2Y}{H_2 + Y}\dfrac{cY}{X + cY}, \end{cases}$$

where $p_i = \frac{1}{T_{H_i}}$ is the maximum number of the respective prey the predator can handle in a unit time and $H_i = \frac{1}{a_iT_{H_i}}$ is the semi-saturation density in the conventional Holling Type-II form. This semi-saturation density is defined to be the amount of prey at which the predation rate is at half of its maximum. Using these predation terms and

the logistic model for the growth of the preys gives:

$$\begin{cases} \frac{dX}{d\bar{t}} &= r_1 X\left(1-\frac{X}{K_1}\right) - \frac{p_1 X}{H_1+X}\frac{X}{X+cY}Z \\ \frac{dY}{d\bar{t}} &= r_2 Y\left(1-\frac{Y}{K_2}\right) - \frac{p_2 Y}{H_2+Y}\frac{cY}{X+cY}Z \\ \frac{dZ}{d\bar{t}} &= Z\left(\frac{bp_1 X}{H_1+X}\frac{X}{X+cY} + \frac{cbp_2 Y}{H_2+Y}\frac{cY}{X+cY}\right) - dZ, \end{cases} \tag{1}$$

where r_i is the maximum reproductive rate for the respective prey, K_i is the carrying capacity for the respective prey, d is the death rate of the predator, and b is the birth to consumption ratio for the predator.

3 Scaling the Model

To analyze the model mathematically, Eq.1 is non-dimensionalized, which reduces the system to a minimum number of parameters. Using the same scaling ideas as [2] and using the following substitutions for variables and parameter values: $x = \frac{X}{K_1}$, $y = \frac{Y}{K_2}$, $z = \frac{p_1 Z}{r_1 K_1}$, $t = bp_1\bar{t}$, $\zeta = \frac{bp_1}{r_1}$, $\epsilon = \frac{bp_1}{r_2}$, $\beta_i = \frac{H_i}{K_i}$, $\sigma = \frac{cK_2}{K_1}$, $\mu = \frac{cp_2 r_1}{p_1 r_2}$, $\nu = \frac{c^2 p_2 K_2}{p_1 K_1}$, and $\delta = \frac{d}{bp_1}$ gives the following dimensionless form of Eq.1:

$$\begin{cases} \zeta\dot{x} &= x\left(1-x-\frac{x}{(\beta_1+x)(x+\sigma y)}z\right) &= xf(x,y,z) \\ \epsilon\dot{y} &= y\left(1-y-\frac{\mu y}{(\beta_2+y)(x+\sigma y)}z\right) &= yg(x,y,z) \\ \dot{z} &= z\left(\frac{x^2}{(\beta_1+x)(x+\sigma y)} + \frac{\nu y^2}{(\beta_2+y)(x+\sigma y)} - \delta\right) &= zh(x,y). \end{cases} \tag{2}$$

The prey density of X is scaled against its carrying capacity, K_1, leaving x as a dimensionless scalar. Similarly, the prey density of Y is scaled against its carrying capacity, K_2, leaving y as a dimensionless scalar. It seems reasonable from a biological viewpoint to expect that the carrying capacity for Z will be approximately the population at which the maximum predator capture rate for X is equal to the maximum growth rate of the prey, $r_1 K_1$. The predator Z is therefore scaled against its predation capacity, $\frac{r_1 K_1}{p_1}$, on X. The parameters β_1 and β_2 are the ratios of the semi-saturation constants of the predator versus the carrying capacity of the respective preys. They are dimensionless constants in the scaled system. Since a decent predator is expected to reach half of its maximum predation rate before its prey reaches its capacity, it is assumed for this paper that $0 < \beta_i < 1$. The parameter δ is the relative death rate. It is the ratio of the predator's death rate to its maximum birth rate without prey Y. The parameters $\frac{1}{\zeta}$ and $\frac{1}{\epsilon}$ are the relative maximum reproductive rates of X and Y to Z, i.e. the XZ-prolificity and the YZ-prolificity.

4 Nullclines

The discussion begins by considering the nullclines $xf(x,y,z) = 0$, $yg(x,y,z) = 0$, and $zh(x,y,z) = 0$. Solving these equations gives:

$$\begin{array}{lllll} x\text{-nullclines:} & x = 0 & \text{and} & z = \phi(x,y) = \frac{(1-x)(\beta_1+x)(x+\sigma y)}{x} \\ y\text{-nullclines:} & y = 0 & \text{and} & z = \varphi(x,y) = \frac{(1-y)(\beta_2+y)(x+\sigma y)}{\mu y} \\ z\text{-nullclines:} & z = 0 & \text{and} & \frac{x^2}{(\beta_1+x)(x+\sigma y)} + \frac{\nu y^2}{(\beta_2+y)(x+\sigma y)} - \delta = 0. \end{array}$$

A nontrivial x-nullcline is seen in Fig.1(a), a nontrivial y-nullcline is seen in Fig.1(b), and a nontrivial z-nullcline is seen in Fig.1(c). An arrangement of the three nontrivial nullclines is seen in Fig.1(d). The nontrivial x-nullcline $f = 0$ is the carrying capacity for prey x when y and z are fixed. Below $f = 0$, $\dot{x} > 0$ so the population of x is increasing with time. Above $f = 0$, $\dot{x} < 0$ so the population of x is decreasing with time. This means that with fewer predators, the prey is allowed to recover and expand in population and with either an excessive amount of prey or an excessive amount of predator, the prey must be in decline. For fixed y and z, the x-population will flow to the x-nullcline surface $f = 0$. Similarly, below the nontrivial y-nullcline surface $g = 0$, prey y is increasing in population and above it prey y is decreasing. On the origin side of the nontrivial z-nullcline $h = 0$, there are insufficient amounts of the preys as $\dot{z}$ is negative so the population of the predator is decreasing. On the other side of the nontrivial z-nullcline $h = 0$, the predator population is increasing.

5 Subsystem Dynamics

5.1 X-Z Dynamics

To simplify the analysis, the case when there are no prey y is considered first. This reduces the equations to the traditional two-dimensional system:

$$\left\{ \begin{array}{rcl} \zeta\dot{x} &=& x\left(1 - x - \frac{z}{\beta_1+x}\right) \\ \dot{z} &=& z\left(\frac{x}{\beta_1+x} - \delta\right) \end{array} \right. \begin{array}{l} = \; xf(x,0,z) \\ = \; zh(x,0). \end{array} \tag{3}$$

Two configurations of the x and z-nullclines are shown in Fig.2(b-c).

The parameter ζ is a time scale parameter. If ζ is small, x changes much faster than z does. This is often the case in predator-prey systems. For any initial condition starting off the nullclines, the solution will quickly approach an x-nullcline, virtually horizontally. Once it reaches an x-nullcline, $\dot{x}$ will be nearly zero so the solution now has a chance to develop in the z-direction. It will do this while staying near the x-nullcline.

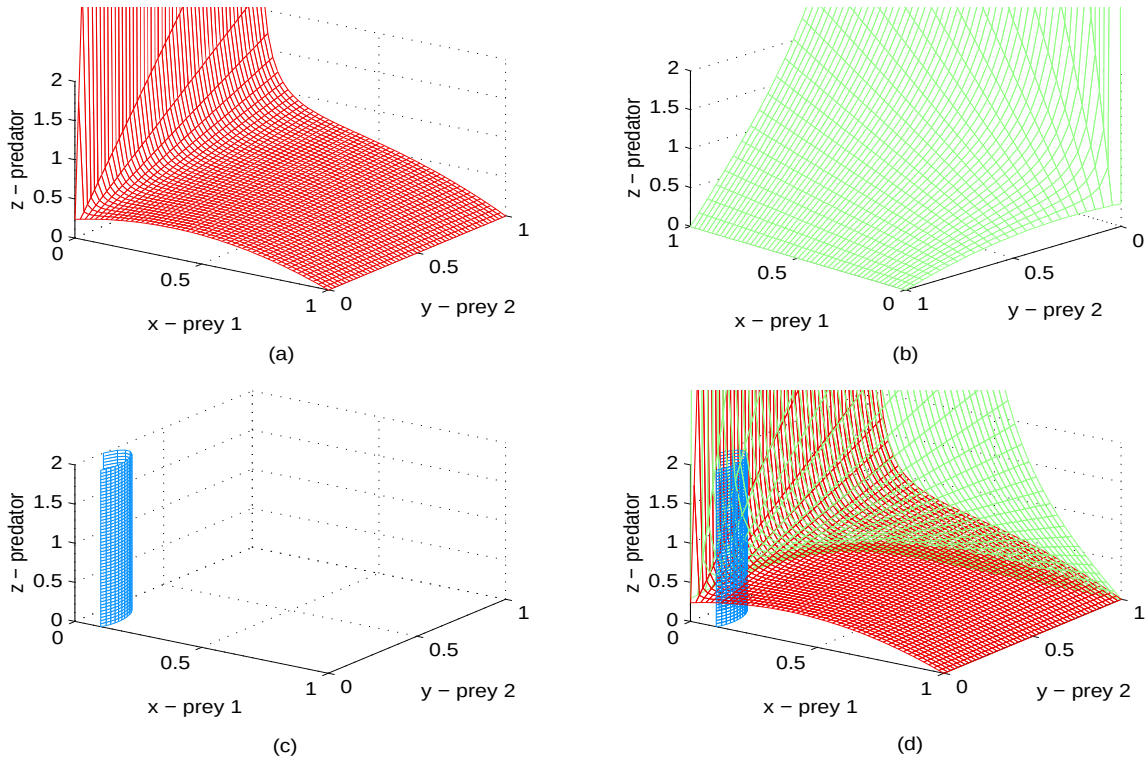

Figure 1: (a) x-nullcline, (b) y-nullcline, (c) z-nullcline, (d) x, y, and z-nullclines.

To determine the orbit of the solutions for small ζ, singular perturbation analysis is used to separate the fast and the slow time scales. For the faster time scale, time is rescaled and reassigned as $t := \frac{t}{\zeta}$ to get:

$$\begin{cases} \dot{x} &= xf(x,0,z) \\ \dot{z} &= \zeta z h(x,0). \end{cases}$$

To isolate the effects of the fast flow, let $\zeta = 0$. This gives a system:

$$\begin{cases} \dot{x} &= xf(x,0,z) \\ \dot{z} &= 0, \end{cases}$$

which will be referred to as the fast subsystem. This fast flow (i.e. orbits of the fast subsystem) is shown in Fig.2(a). Notice that this flow develops only in the x-direction.

To get the slow flow for the predator, let $\zeta = 0$ in Eq.3. The system corresponding to the slow flow, the slow subsystem, is:

$$\begin{cases} 0 &= xf(x,0,z) \\ \dot{z} &= zh(x,0). \end{cases}$$

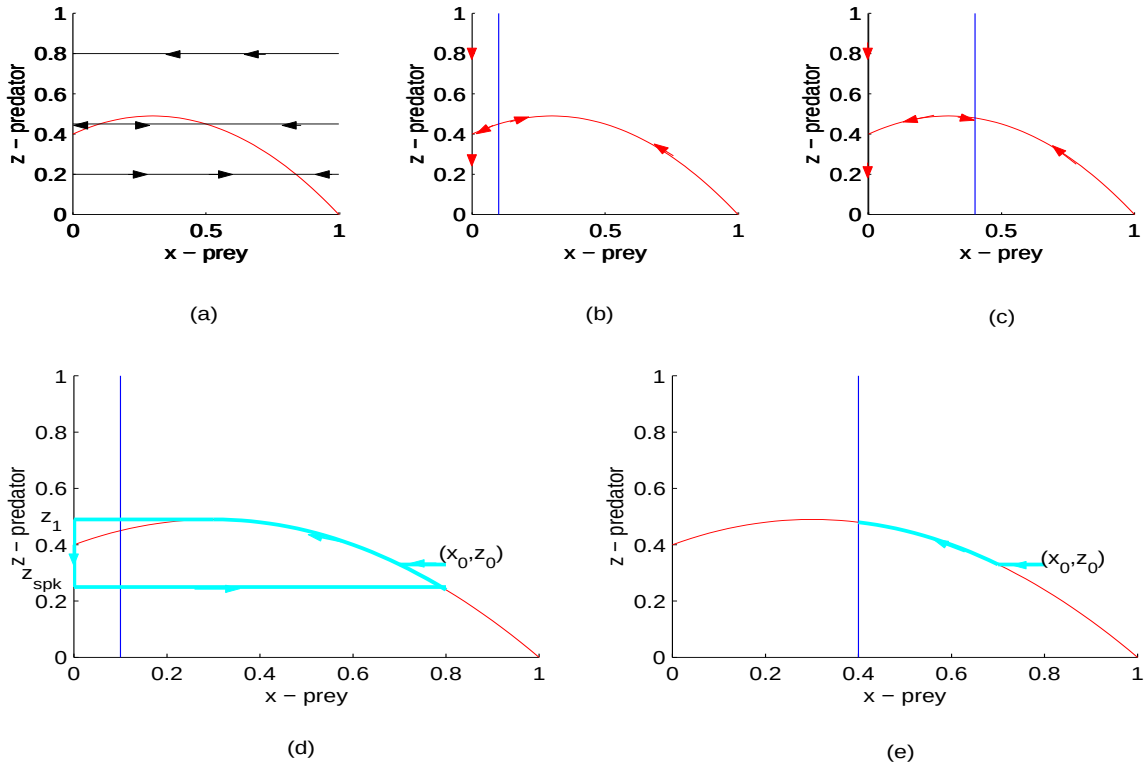

Figure 2: (a) Fast flow, (b) Slow flow, (c) Slow flow, (d) Singular orbit for limit cycle, (e) Singular orbit for equilibrium point (x-nullcline is red, z-nullcline is blue).

This slow flow happens on the slower time scale and develops only along the x-nullclines. The slow flow is shown in Fig.2(b-c) for different configurations of the nullclines.

Concatenating orbits from the fast and slow subsystems yields *singular orbits*. The singular orbit will end up at either an equilibrium point or a limit cycle, depending on whether the z-nullcline $h = 0$ is to the left or to the right of the maximum of the x-nullcline $f = 0$. For small ζ, it can be shown that the orbit is near the singular orbit. In particular, if the singular flow admits an equilibrium or a limit cycle, then so does the flow for small ζ.

Fig.2(d) shows the case of a limiting cycle. An orbit that is to the right of the z-nullcline after the fast subsystem follows the shape of the x-nullcline parabola. When it reaches the maximum at the point $\left(\frac{1-\beta_1}{2}, \frac{(1+\beta_1)^2}{4}\right)$, it jumps over to the z-axis following the flow lines of the fast subsystem. The orbit then travels down the z-axis following the slow subsystem. The orbit begins to feel the effect of the rightward pull by the fast orbit once it passes the transcritical point, $(0, \beta_1)$. The transcritical point

is where the x-nullclines intersect and change stability. However, it remains on the unstable z-axis for some time until it reaches a point z_{spk}, which can be determined explicitly. The fact that the singular orbit does not immediately jump to a fast orbit at the transcritical point even though the z-axis becomes unstable there, is known as Pontryagin's delay of loss of stability [8],[7],[6],[4].

To calculate the value of z_{spk} where the the singular orbit jumps to a fast orbit, it is necessary to know the z-coordinate where the orbit first hits the z-axis, which will be called z_1. For the singular limit cycle, z_1 will be the same as that of the z-coordinate of the maximum of the parabola $f = 0$. Thus, $z_1 = \frac{(1+\beta_1)^2}{4}$. z_{spk} is uniquely determined by z_1 as the value that satisfies $\int_{z_1}^{z_{spk}} \frac{f(0,z)}{zh(0,z)} dz = 0$ [4]. Notice that $\frac{f(0,z)}{zh(0,z)}$ is negative for z below β_1 and positive above β_1. The negative area from z_{spk} to β_1 cancels with the positive area from β_1 to z_1. More specifically,

$$\begin{aligned} 0 &= \int_{z_1}^{z_{spk}} \frac{f(0,z)}{zh(0,z)} dz \\ &= \int_{z_1}^{z_{spk}} \frac{1 - \frac{z}{\beta_1}}{-z\delta} dz \\ &= \frac{1}{\delta}(\ln z_1 - \beta_1 z_1 - (\ln z_{spk} - \beta_1 z_{spk})). \end{aligned}$$

This leads to:

$$\ln z_1 - \beta_1 z_1 = \ln z_{spk} - \beta_1 z_{spk}.$$

In the limit cycle case, x goes through a phase of crash-recovery-outbreak. It crashes at z_1 and outbreaks at z_{spk}.

Fig.2(e) shows the case of the stable equilibrium. All solutions will go to the equilibrium point by first following the fast system over to the $f = 0$ parabola. Then the solution will follow the parabola until it reaches the equilibrium point $\left(\frac{\beta_1\delta}{1-\delta}, \frac{\beta_1 - \beta_1\delta - \delta\beta_1^2}{(1-\delta)^2}\right)$.

5.1.1 Addition of Y

The model changes when a fixed amount of prey y is added to the system. For $y = 0$, the per capita rate, $\frac{1}{x}\frac{dx}{dt}$, at $x = 0$ is $f(0,0,z) = (1 - \frac{z}{\beta_1})$, which is greater than zero for $z < \beta_1$ and less than zero for $z > \beta_1$. This implies that the x-nullcline $x = 0$ is stable for $z > \beta_1$ and unstable for $z < \beta_1$. However, for $y > 0$, $f(0,y,z) = 1$, which is always greater than zero. This implies that for $y > 0$ the x-nullcline $x = 0$ is always unstable. This is also seen in the fact that the three-dimensional x-nullcline $f = 0$ is asymptotic to the $x = 0$ surface for all values of $y > 0$ as seen in Fig.1(a). This occurs because of the density dependent relationship in the predation of x and y. The predator z focuses its attention more on y when the x-population is small.

This prevents the x-population from dying off as long as there are prey y. The stable asymptotic sheet of the x-nullcline surface $f = 0$, which represents the predator z and prey y mediated carrying capacity of x, pulls away from the z-axis as y increases. The predator z is drawn away from prey x by the presence of the large y-population.

5.1.2 Crash and Outbreak Fold on the X-nullcline

There may develop a crash fold and an outbreak fold on the x-nullcline surface $f = 0$. In the two-dimensional case, the singular orbit travels up the stable branch of the x-nullcline, hits the maximum and jumps via the fast flow to $x = 0$. This phenomenon is called a crash. In particular, a crash in x occurs any time the x-population hits a local maximum on the x-nullcline surface and jumps to another branch of the x-nullcline surface, which is either near zero or at zero. More technically, a crash point, (x_{cf}, y_{cf}, z_{cf}), occurs on the x-nullcline surface if the following three conditions are satisfied: (1) For $x_0 > x_{cf}$, y_{cf} and z_{cf} fixed, $x(t, x_0, y_{cf}, z_{cf}) \to x_{cf}$ and for $x_0 < x_{cf}$, $x(t, x_0, y_{cf}, z_{cf}) \to \underline{x}(y_{cf}, z_{cf}) < x_{cf}$ where $f(\underline{x}, y_{cf}, z_{cf}) = 0$ or $\underline{x} = 0$ and $\underline{x}$ is a value of x which is less than x_{cf}. (2) For $z_0 > z_{cf}$, $x(t, x_0, y_{cf}, z_0) \to \underline{x}(y_{cf}, z_0) < x_{cf}$ such that $f(\underline{x}, y_{cf}, z_0) = 0$ or $\underline{x} = 0$. (3) For $y_0 > y_{cf}$, there is always $x_0 < x_{cf}$ and certainly all $x_0 > x_{cf}$ such that $x(t, x_0, y_0, z_{cf}) \to \bar{x}(y_0, z_{cf}) > x_{cf}$, where $\bar{x}$ is a value of x greater than x_{cf}, so that $f(\bar{x}, y_{cf}, z_{cf}) = 0$. In the three-dimensional case, there will be a whole line segment of crash points, which will be called a crash fold. As y_{cf} increases along the crash fold, x_{cf} decreases. This shifting takes place because an increase in the population of one prey alleviates the predation pressure on the other prey.

The opposite of crashing behavior can also occur. This is referred to as outbreaks. The outbreak point in the two-dimensional system is just the transcritical point. An outbreak in x occurs any time the x-population hits a local minimum on the x-nullcline surface and jumps to another branch of the x-nullcline surface. An outbreak point, (x_{of}, y_{of}, z_{of}), occurs if the following three conditions hold: (1) For $x_0 < x_{of}$, y_{of} and z_{of} fixed, $x(t, x_0, y_{of}, z_{of}) \to x_{of}$ and for $x_0 > x_{of}$, $x(t, x_0, y_{of}, z_{of}) \to \bar{x}(y_{of}, z_{of}) > x_{of}$ with $f(\bar{x}, y_{of}, z_{of}) = 0$. (2) For $z_0 < z_{of}$, $x(t, x_0, y_{of}, z_0) \to \bar{x}(y_{of}, z_0) > x_{of}$ such that $f(\bar{x}, y_{of}, z_0) = 0$. (3) For $y_0 > y_{of}$, then $x(t, x_{of}, y_0, z_{of}) \to \bar{x}(y_0, z_{of}) > x_{of}$ with $f(\bar{x}, y_0, z_{of}) = 0$. The last condition means that along the outbreak fold, both x and z increase as y increases. Hence, the outbreak fold and the crash fold will eventually meet as y increases. Together, they form a curve on the x-nullcline $f = 0$, which will simply be called the x-nullcline fold.

To calculate the location of the crash and outbreak folds, the surface $f(x, y, z) = 0$ is represented as a function $z = \phi(x, y)$. The crash fold and outbreak fold are the local x-maximum and x-minimum, respectively, of $z = \phi(x, y)$. They are cal-

culated by solving $\frac{\partial \phi}{\partial x}(x,y) = 0$. There will be two solutions: $(x,y) = (x_{cf}, y_{cf})$ and $(x,y) = (x_{of}, y_{of})$. By implicit differentiation of $f(x,y,\phi(x,y)) \equiv 0$ in x, $f_x(x,y,\phi) + f_z(x,y,\phi)\phi_x(x,y) = 0$ at (x_{cf}, y_{cf}, z_{cf}) or (x_{of}, y_{of}, z_{of}). Since $\phi_x = 0$ at these points, $f_x = 0$ at these points. Then the equations for the fold points are:

$$\begin{cases} f(x,y,z) &= 0 \\ f_x(x,y,z) &= 0. \end{cases} \tag{4}$$

From these two equations and three unknowns, y and z can be calculated as $y = \psi(x) = -x^2 \frac{\beta_1 + 2x - 1}{\sigma(\beta_1 + x^2)}$ and $z = \theta(x) = \phi(x, \psi(y))$. $\psi(x)$ is a projection onto the xy-plane of the x-nullcline fold. The x-nullcline fold is seen in Fig.3(a).

The fold of the parabola-like curve ψ is where $\frac{dy}{dx} = \psi'(x) = 0$, which is the point where the outbreak fold and the crash fold meet. Since $f(x, \psi(x), \theta(x)) = 0$, $f_x(x, \psi(x), \theta(x)) = 0$, $\psi_x = 0$, and $\theta_x = 0$, then $f_{xx} + f_{xy}\psi_x + f_{xz}\theta_x = 0$. The point where the fold lines meet can then be calculated by solving:

$$\begin{cases} f(x,y,z) &= 0 \\ f_x(x,y,z) &= 0 \\ f_{xx}(x,y,z) &= 0. \end{cases}$$

This point occurs at $x_{cof} = \beta_1^{\frac{1}{3}} - \beta_1^{\frac{2}{3}}$, the maximum of the parabola-like x-nullcline fold $y = \psi(x)$. This implies that the fold is a crash fold if $x > x_{cof}$ and an outbreak fold if $x < x_{cof}$.

At the crash fold the population of x will decrease to near zero where it will hit the stable asymptotic steady state of the x-nullcline surface $f = 0$, i.e. the part of $f = 0$ near $x = 0$. If there are no prey y the x-population will go to $x = 0$ as in the system in Eq.3 where $x = 0$ is stable. For a large enough population of y, the x-fold line will disappear. This occurs when y is greater than the maximum y-value, y_{cof}, of $y = \psi(x_{cof})$ because the predator z will, due to its density dependent predation, focus on hunting the more populous prey y. In this case, $f = 0$ is monotone for $y > y_{cof}$ and hence has no local maximum or minimum. The population of x will neither crash nor outbreak as the x-nullcline $f = 0$ is always stable for $y > y_{cof}$. The x-population will decrease to the stable x-nullcline $f = 0$ for $z > \phi(x,y)$ and increase to the stable x-nullcline $f = 0$ for $z < \phi(x,y)$.

The region of the x-nullcline surface $f = 0$ bounded by the crash and the outbreak folds is the *threshold region*. The threshold region is an unstable branch of the x-nullcline $f = 0$. Given y_0 and z_0, x_{th} is the threshold if for $x_0 < x_{th}$, $x(t, x_0, y_0, z_0) \to \underline{x}(y_0, z_0) < x_{th}$ and for $x_0 > x_{th}$, $x(t, x_0, y_0, z_0) \to \bar{x}(y_0, z_0) > x_{th}$ where $f(\bar{x}, y_0, x_0) = 0$ and $f(\underline{x}, y_0, z_0) = 0$ or $\underline{x} = 0$.

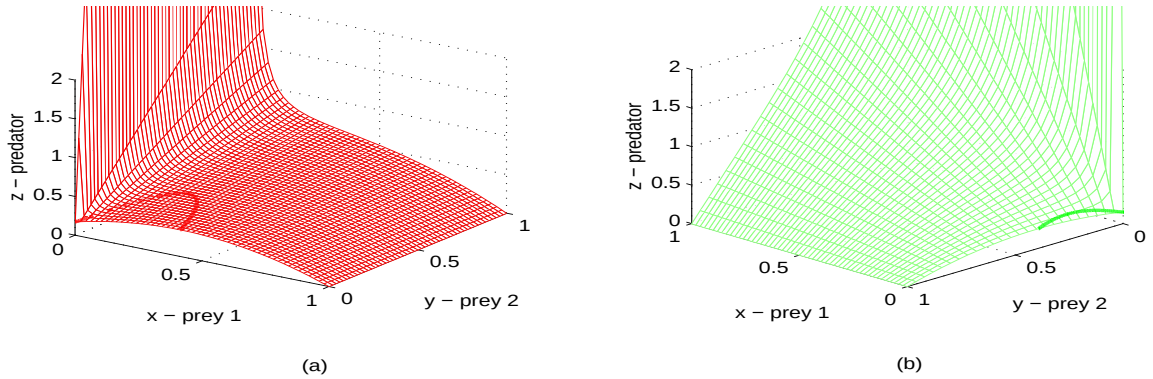

Figure 3: (a) x-nullcline fold, (b) y-nullcline fold.

5.2 Y-Z Dynamics

The y-nullcline surface $g = 0$ is very similar to the x-nullcline surface $f = 0$ and the two-dimensional y-z system behaves similarly to the x-z system described above. Therefore, only the main points will be highlighted in this section. With $x = 0$, the two-dimensional y-z system is:

$$\begin{cases} \epsilon \dot{y} &= y\left(1 - y - \frac{\mu}{\sigma(\beta_2+y)}z\right) &= yg(0,y,z) \\ \dot{z} &= z\left(\frac{\nu y}{\sigma(\beta_2+y)} - \delta\right) &= zh(0,y). \end{cases} \tag{5}$$

The parameter ϵ is now the time scale parameter and the system can be analyzed using singular perturbation analysis similar to the analysis of Eq.3. There will either be an equilibrium point or a limit cycle.

The maximum of the y-nullcline parabola $g = 0$ is $\left(0, \frac{1-\beta_2}{2}, \frac{\sigma(1+\beta_2)^2}{4\mu}\right)$ and the equilibrium point is now $\left(0, \frac{\beta_2\delta\sigma}{\nu-\delta\sigma}, \frac{\nu^2\sigma\beta_2-\delta\sigma^2\beta_2\nu-\delta\beta_2^2\sigma^2\nu}{\mu(\nu-\delta\sigma)^2}\right)$. When a fixed amount of x is added, the y-nullcline $y = 0$ is always unstable. The y-nullcline $g = 0$ has outbreak and crash points similar to those of the x-nullcline $f = 0$. The y-nullcline fold (the union of the outbreak and crash points) is calculated by solving:

$$\begin{cases} g(x,y,z) &= 0 \\ g_y(x,y,z) &= 0 \end{cases} \tag{6}$$

for x which gives $x = \chi(y) = -\sigma y^2 \frac{\beta_2+2y-1}{\beta_2+y^2}$. The y-nullcline fold is seen in Fig.3(b). There is a point on the fold at $y = y_{cog}$ where $g_{yy} = 0$. At this point, the fold changes from being a local maximum in the y-nullcline surface $g = 0$ to being a local minimum. The point where the y-nullcline fold changes from a crash fold to an outbreak fold is $y_{cog} = \beta_2^{\frac{1}{3}} - \beta_2^{\frac{2}{3}}$. It is a crash fold if $y > y_{cog}$ and an outbreak fold if $y < y_{cog}$. The

y-nullcline $g = 0$ has a threshold region bounded by the crash and outbreaks folds. This region is analogous to the threshold region on the x-nullcline $f = 0$.

5.3 X-Y Dynamics

In the absence of predator z, the populations of preys x and y will increase to their carrying capacities at the point $(1, 1, 0)$. For a fixed value of z, the intersection of the x and y-nullcline surfaces is the carrying capacity for the individual prey. As predator z is added, the individual carrying capacities for x and y decrease from the point $(1, 1, 0)$ along the intersection line of the x and y-nullclines:

$$\begin{cases} f(x,y,z) &= 1 - x - \frac{x}{(\beta_1+x)(x+\sigma y)}z &= 0 \\ g(x,y,z) &= 1 - y - \frac{\mu y}{(\beta_2+y)(x+\sigma y)}z &= 0. \end{cases}$$

Eliminating z from both equations gives $(1 - x)(\beta_1 + x)\mu y = x(1 - y)(\beta_2 + y)$. This equation is quadratic in both x and y so x can be solved as a function of y, $x = \xi(y)$, which is monotone increasing because as x decreases the predator mediated joint prey capacities decrease for both.

The xy-intersection line and the x and y-fold lines are now looked at by projecting them onto the xy-plane as seen in Fig.4(a). Remember that $\psi(x)$ and $\chi(y)$ are the projections of the x and y-nullcline folds, respectively. For $y < \psi(x)$, the x-nullcline $f = 0$ is unstable and the x-population will eventually jump, increasing if it reaches the outbreak fold and decreasing if it reaches the crash fold. The x-nullcline $f = 0$ is stable for $y > \psi(x)$. For $x > \chi(y)$, the y-nullcline $g = 0$ is stable. For $x < \chi(y)$, the y-nullcline $g = 0$ is unstable and the y population will jump increasing if it reaches the outbreak fold and decreasing if it reaches the crash fold. This paper will focus on when the x-fold, the y-fold and the xy-intersection line only intersect at $(0, 0, 0)$ as this seems to be the most common configuration for reasonable parameter values.

There is also a joint xy-crash point, xy_{crash}, that occurs at the maximum z-value of the xy-intersection line. This point is shown in Fig.4(a) as well as in the xz-plane in Fig.4(b) and the yz-plane in Fig.4(c). The xy-intersection line is unstable for x and y-values on the xy-intersection line for which x and y are less than xy_{crash}. If the orbit hits xy_{crash}, both x and y will crash.

5.4 Z-nullcline

The nontrivial z-nullcline, $h(x, y) = \frac{x^2}{(\beta_1+x)(x+\sigma y)} + \frac{\nu y^2}{(\beta_2+y)(x+\sigma y)} - \delta = 0$ is quadratic in x and y and so can be expressed in two branches. The first branch is solved as $y = y(x)$ for $0 \leq x \leq \frac{\delta\beta_1}{1-\delta}$ with a maximum y-value at $y = y_{zmax}$ and the second branch as $x = x(y)$ for $x \geq \frac{\delta\beta_1}{1-\delta}$ with a maximum x-value at $x = x_{zmax}$. It is independent of z.

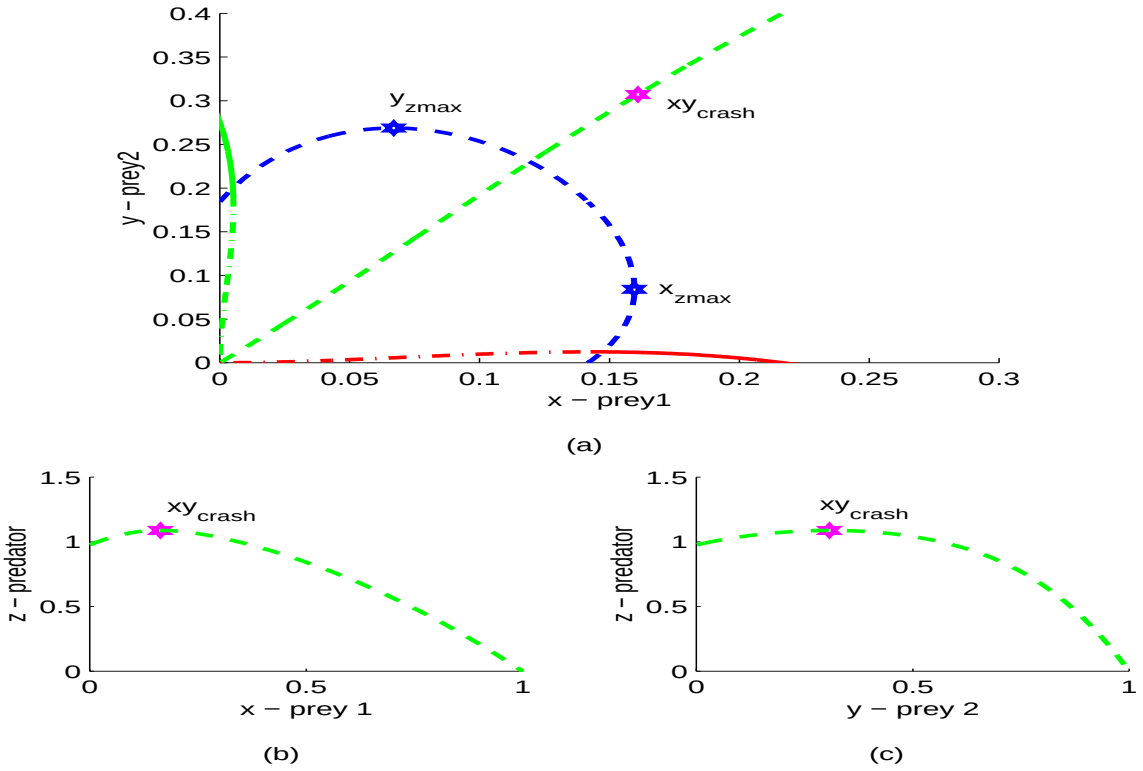

Figure 4: (a) The x-nullcline fold is red with crash portion a solid line and outbreak portion a dash-dotted line. The y-nullcline fold is green with solid crash line and a dash-dotted outbreak line. The xy-intersection is the green dashed line and the z-nullcline is the blue dashed line. (b) The projection of the xy-intersection line in the xz-plane. (c) The projection of the xy-intersection line in the yz-plane.

The nontrivial z-nullcline $h = 0$ is the division between where the population of the predator z is decreasing and where the population is increasing. This is representative of the fact that if there are few prey the predator population will be decreasing. When there are enough prey, the predator population will be increasing. The z-nullcline curve represents the minimal amount of preys required to sustain a growing z.

The projection of the z-nullcline in the xy-plane is seen in Fig.4(a). There are four cases for the configuration depending on whether y_{zmax} and/or x_{zmax} lie in the first quadrant. In the case shown, both y_{zmax} and x_{zmax} are in the first quadrant. As the population of y increases from zero, z is distracted by y so a smaller portion of time is spent preying on x. As a consequence, at a constant z-level a larger population of x is required to make it easier for z to sustain the minimal amount of growth before y is sufficient enough to reward the predator's attention. This occurs for $0 < y < \tilde{y}$, where $\tilde{y}$ is the y-coordinate of the x_{zmax} point, i.e. $x_{zmax} = x(\tilde{y})$. Similarly, as x

increases from zero to $\tilde{x}$, the x-coordinate of the y_{zmax} point, i.e. $y_{zmax} = y(\tilde{x})$, z is distracted by x so a larger population of y is needed to maintain the minimal amount for z's growth. This causes the z-nullcline $h = 0$ to bulge out. In the portion of $h = 0$ where $x > \tilde{x}$ and $y > \tilde{y}$, an increase in x with fixed z leads to a decrease in y and an increase in y with fixed z leads to a decrease in x. In this case, the predator will focus more on the more abundant prey making the other prey less necessary. Fewer of the less abundant prey are needed to maintain the minimal amount for the growth of z.

5.5 Predator Efficiency

The predator is defined to be x-efficient when the z-nullcline $h = 0$ intersects the x-nullcline $f = 0$ to the left of the maximum of $f(x, 0, z) = 0$, which is the unstable portion of the x-nullcline surface. The maximum of $f = 0$ occurs at $x = \frac{1-\beta_1}{2}$ and the x-intercept of the z-nullcline $h = 0$ is $x = \frac{\beta_1\delta}{1-\delta}$. Therefore, the predator is defined to be x-efficient if and only if $\frac{\beta_1\delta}{1-\delta} < \frac{1-\beta_1}{2}$. Solving this for β_1 implies that the predator is x-efficient for $\beta_1 < \frac{1-\delta}{1+\delta}$. The predator is said to be weak if it is not efficient. Hence, the condition for the predator to be x-weak is $\frac{\beta_1\delta}{1-\delta} > \frac{1-\beta_1}{2}$ or equivalently $\beta_1 > \frac{1-\delta}{1+\delta}$. When the predator is x-weak, the z-nullcline intersects the $f = 0$ surface to the right of the maximum of the parabola $f(x, 0, z)$, which is the stable portion of the x-nullcline.

The predator is y-efficient when the z-nullcline $h = 0$ intersects the the y-nullcline $g = 0$ on the unstable portion. The maximum of the y-nullcline $g(0, y, z) = 0$ parabola occurs at $y = \frac{1-\beta_2}{2}$ and the y-intersection of the z-nullcline $h = 0$ is $y = \frac{\delta\sigma\beta_2}{\nu-\delta\sigma}$. The predator z is y-efficient for $\frac{\delta\sigma\beta_2}{\nu-\delta\sigma} < \frac{1-\beta_2}{2}$. Solving this for β_2 gives the condition for the predator to be y-efficient as $\beta_2 < \frac{1-\frac{\delta\sigma}{\nu}}{1+\frac{\delta\sigma}{\nu}}$. The predator z is weak if it is not efficient, so it is y-weak if $\frac{\delta\sigma\beta_2}{\nu-\delta\sigma} > \frac{1-\beta_2}{2}$ or equivalently $\beta_2 > \frac{1-\frac{\delta\sigma}{\nu}}{1+\frac{\delta\sigma}{\nu}}$. This is when the z-nullcline intersects $g(0, y, z) = 0$ on the stable portion of the y-nullcline.

There are four main cases to consider for the intersection of the z-nullcline with the x and y-nullclines. The predator can be x-efficient or x-weak and y-efficient or y-weak. The cases are: z is x-efficient and y-efficient, x-efficient and y-weak, x-weak and y-efficient, or x-weak and y-weak. This paper will focus on the x-efficient, y-efficient case, which has the most interesting behavior.

6 Behavior of the System for the X-efficient, Y-efficient Case

6.1 X-Z Dynamics

Consider the behavior for x and z first when $y = 0$ as in Eq.3 and z is x-efficient. The three possible equilibrium points are $(0,0,0)$, $(1,0,0)$, and $\left(\frac{\beta_1\delta}{1-\delta}, 0, \frac{\beta_1-\beta_1\delta-\delta\beta_1^2}{(1-\delta)^2}\right)$. Eq.3 is linearized and the eigenvalues of the Jacobian are determined. From this, it is determined that $(0,0,0)$ is always a saddle. It is only reached if there are no prey initially. $(1,0,0)$ is a stable equilibrium if $\frac{\delta\beta_1}{1-\delta} > 1$. This corresponds to the case when the z-nullcline is to the right of $x = 1$ so that there are only two equilibria. In this case, the death rate of the predator is so high that its population cannot be sustained, even if the prey are at their carrying capacity. $(1,0,0)$ is a saddle if $\frac{\delta\beta_1}{1-\delta} < 1$, and in this case, $(1,0,0)$ is only reached if there are no predators initially. The equilibrium $\left(\frac{\beta_1\delta}{1-\delta}, 0, \frac{\beta_1-\beta_1\delta-\delta\beta_1^2}{(1-\delta)^2}\right)$ can be a stable or unstable spiral. It is stable if $\beta_1 > \frac{1-\delta}{1+\delta}$, which means the predator is x-weak. In this case, starting with a positive amount of z and x means the orbit will approach this equilibrium. If instead the predator is x-efficient, $\beta_1 < \frac{1-\delta}{1+\delta}$, then the z-nullcline lies between $x = 0$ and $x = x_{max} = \frac{1-\beta_1}{2}$ and $\left(\frac{\beta_1\delta}{1-\delta}, 0, \frac{\beta_1-\beta_1\delta-\delta\beta_1^2}{(1-\delta)^2}\right)$ is an unstable spiral. If the parameter β_1 is allowed to change continuously, then as the z-nullcline crosses the line $x = x_{max}$ a Hopf bifurcation occurs. A small periodic orbit appears, encircling the equilibrium. From the Hopf bifurcation theorem alone, it is not known if this periodic orbit persists after the z-nullcline passes farther away to the left of $x = x_{max}$.

The stability of the equilibrium point $\left(\frac{\beta_1\delta}{1-\delta}, 0, \frac{\beta_1-\beta_1\delta-\delta\beta_1^2}{(1-\delta)^2}\right)$ is of most interest. From calculating the eigenvalues of the linearized system, the following conclusions are reached: (1) the equilibrium state is locally stable if and only if the predator z is weak, and (2) if z is efficient, then a limit cycle occurs around the unstable equilibrium point which is initially induced by a Hopf bifurcation. The global behavior can be determined by:

Theorem (A.N. Kolmogorov, 1936): *If a system of equations:*

$$\begin{cases} \dot{x} = & xf(x,y) \\ & \qquad \textit{for } x \geq 0, y \geq 0. \\ \dot{y} = & yg(x,y), \end{cases}$$

satisfies:

1. $f(0,0) > 0$, $\frac{\partial f}{\partial y} < 0$, $x\frac{\partial f}{\partial x} + y\frac{\partial f}{\partial y} < 0$;
2. $\frac{\partial g}{\partial y} \leq 0$, $x\frac{\partial g}{\partial x} + y\frac{\partial g}{\partial y} > 0$;

3. *There exists constants* $A > 0$, $B > C > 0$ *such that* $f(0, A) = f(B, 0) = g(C, 0) = 0$;

Then there exists either a global stable equilibrium point or a global stable limit cycle.

It is straightforward to verify these conditions for Eq.3 with $A = \beta_1$, $B = 1$, and $C = \frac{\beta_1\delta}{1-\delta}$. Combining this with the local stability result above, concludes that a globally stable limit cycle occurs if and only if the predator z is x-efficient, i.e. where $\beta_1 < \frac{1-\delta}{1+\delta}$.

6.2 Y-Z Dynamics

Now consider the case when the predator is y-efficient and $x = 0$ as in Eq.5. The stability of the point $\left(0, \frac{\beta_2\delta\sigma}{\nu-\delta\sigma}, \frac{\nu^2\sigma\beta_2\delta\sigma^2\beta_2\nu-\delta\beta_2^2\sigma^2\nu}{\mu(\nu-\delta\sigma)^2}\right)$ is analyzed using the same methods as above. This analysis shows that there can be either a globally stable equilibrium point or a globally stable limit cycle. The limit cycle occurs if and only if the predator z is y-efficient, i.e. when $\beta_2 < \frac{1-\frac{\delta\sigma}{\mu}}{1+\frac{\delta\sigma}{\nu}}$.

6.3 Singular Perturbation Analysis

Singular perturbation analysis is used to analyze the full three-dimensional system of Eq.2. This isolates the fast, intermediate, and slow time scales. To get the fast subsystem, the equations are rescaled using $\tau = \frac{t}{\zeta}$. Letting $\zeta = 0$ gives the fast subsystem:

$$\left\{\begin{array}{rcccl} \dot{x} & = & xf(x,y,z) & = & x\left(1 - x - \frac{x}{(\beta_1+x)(x+\sigma y)}z\right) \\ \epsilon\dot{y} & = & \zeta y g(x,y,z) & = & 0 \\ \dot{z} & = & \zeta z h(x,y) & = & 0. \end{array}\right. \tag{7}$$

Orbits of the fast subsystem are seen in Fig.5(a). Orbits of this system develop in the x-direction only. All non-equilibrium solutions will quickly approach the stable branches of the x-nullcline. The orbit will jump from an initial condition, (x_0, y_0, z_0), to the stable part of the x-nullcline $f = 0$, or $x = 0$ if $y = 0$. It will do this by decreasing in x if (x_0, y_0, z_0) is above the x-nullcline $f = 0$ and increasing in x if (x_0, y_0, z_0) is below the x-nullcline $f = 0$. The only unstable portion of the x-nullcline $f = 0$ is the threshold region. If the x-population starts on the threshold region it will remain there, but if it starts nearby, the orbit will move away from the threshold region undergoing an outbreak or a crash. Let x_1 be the x-coordinate of the orbit after this first leg of the fast subsystem, so at that point the orbit will be at (x_1, y_0, z_0). An example is seen in Fig.5(d).

Once on the stable portion of the x-nullcline, $\dot{x}$ is zero. Since x is no longer changing, the focus is now on the time scale of prey y. To get this intermediate

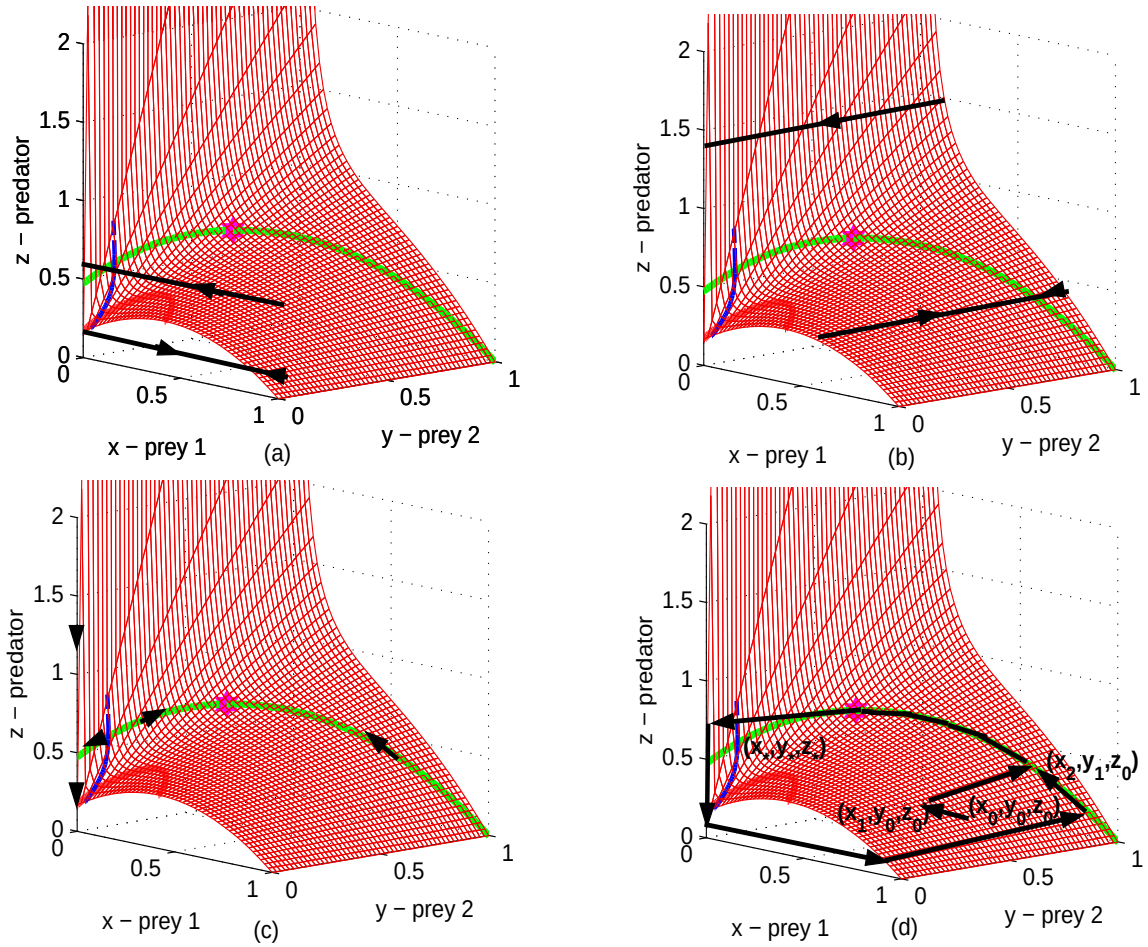

Figure 5: (a) Fast subsystem, (b) Intermediate subsystem, (c) Slow subsystem, (d) Singular orbit analysis.

subsystem, time is rescaled as $t = \frac{\tau}{\epsilon}$. Letting $\zeta = 0 = \epsilon$ gives the intermediate subsystem:

$$\left\{ \begin{array}{rcccl} 0 & = & xf(x,y,x) & = & x\left(1 - x - \frac{x}{(\beta_1+x)(x+\sigma y)}z\right) \\ \dot{y} & = & yg(x,y,z) & = & y\left(1 - y - \frac{\mu y}{(\beta_2+y)(x+\sigma y)}z\right) \\ \dot{z} & = & \epsilon z h(x,y) & = & 0. \end{array} \right. \tag{8}$$

Orbits of this system lie on the x-nullcline as seen in Fig.5(b). Their movement is governed by the position of the orbit compared to the y-nullcline. There are two cases. First, if the orbit on the x-nullcline at (x_1, y_0, z_0) has $x_1 > \xi(y_0)$, where $x = \xi(y)$ is the intersection curve of the x-nullcline $f = 0$ and the y-nullcline $g = 0$, then the orbit will travel toward the stable part of the y-nullcline $g = 0$ in the increasing y-direction until it reaches the xy-intersection line. The second case occurs when

$x_1 < \xi(y_0)$. In this case, the orbit will travel in the decreasing y-direction until it reaches the xy-intersection line or the z-axis. Since it is assumed that the x-fold, y-fold, and xy-intersection line do not intersect, the intermediate subsystem will never hit the threshold region of the y-nullcline. It will lead to the xy-intersection line or the z-axis. An example of the intermediate subsystem for the case where the orbit arrives on the xy-intersection line at the point (x_2, y_1, z_0) is seen in Fig.5(d) for the case where $x_1 > \xi(y_0)$.

The slow subsystem is considered next. Since x and y are no longer changing, the focus is on z. The slow subsystem is determined by setting $\zeta = 0 = \epsilon$, which gives:

$$\begin{cases} 0 = xf(x,y,x) = x\left(1 - x - \frac{x}{(\beta_1+x)(x+\sigma y)}z\right) \\ 0 = yg(x,y,z) = y\left(1 - y - \frac{\mu y}{(\beta_2+y)(x+\sigma y)}z\right) \\ \dot{z} = zh(x,y). \end{cases} \tag{9}$$

Orbits of this system lie on the xy-intersection line and the z-axis as seen in Fig.5(c). The xy-intersection line intersects the z-nullcline at a point, call it (x_*, y_*, z_*). If (x_2, y_1, z_0) is to the right of the z-nullcline, then the orbit will travel along the xy-intersection line in the increasing z-direction toward xy_{crash}. If the orbit arrives at xy_{crash}, then the populations of x and y will crash toward zero. Once at the z-axis, the orbit will decrease in z. Then the population of x will outbreak following the fast subsystem. A cycle will form and (x_*, y_*, z_*) is unstable. If the orbit reaches (x_*, y_*, z_*) before the xy_{crash}, then (x_*, y_*, z_*) is a stable equilibrium. For x_2 to the left of the z-nullcline $h = 0$, the orbit will travel along the xy-intersection line in the decreasing z-direction to the z-axis. An outbreak of x will occur following the fast subsystem. An example of a singular orbit for the limit cycle case is seen in Fig.5(d).

6.3.1 Stable Limit Cycle

Fig.6(a) shows a numerical simulation for a stable limit cycle near the singular stable limit cycle. All simulations are done on Matlab using the numerical solver ode15s with double precision and the BDF (backward differentiation formula) option. In the simulation, $0 < \zeta \ll 1$ and $0 < \zeta \ll \epsilon \ll 1$. Fig.6(b) shows the folds and intersection lines for this case. The populations of x and y will jointly crash at the xy-crash point and then the population of x will outbreak.

6.3.2 Stable Equilibrium

An unexpected behavior is a stable equilibrium point that occurs when z is both x-efficient and y-efficient. Previous analysis shows that limit cycles will occur for the two-dimensional case when z is efficient. It might be expected that this behavior

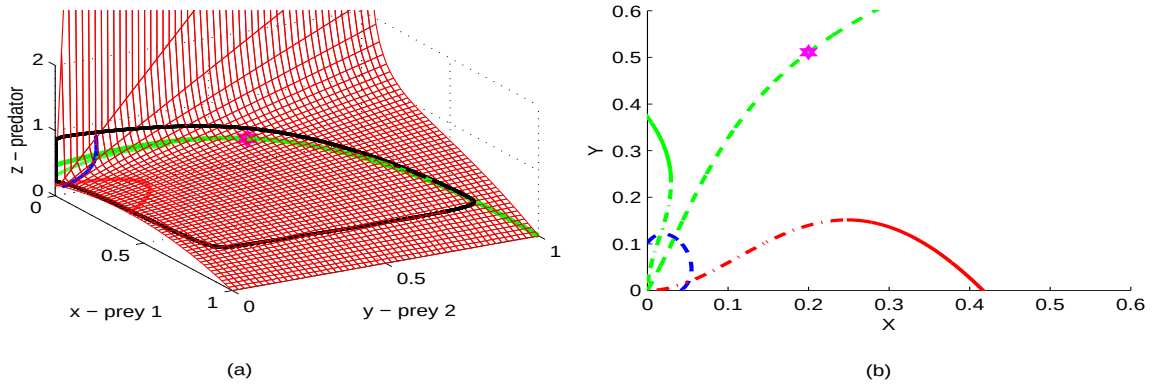

Figure 6: (a) A stable limit cycle with parameter values: $\zeta = .01; \epsilon = .09; \delta = .2; \sigma = .6; \mu = .5; \nu = .42; \beta_1 = (1-\delta)/(1+\delta) - .5; \beta_2 = (1-\delta\sigma/\nu)/(1+\delta\sigma/\nu) - .3$, (b) x-fold, y-fold, xy-nullcline intersection, xy_{crash}, and z-nullcline projected in the xy-plane.

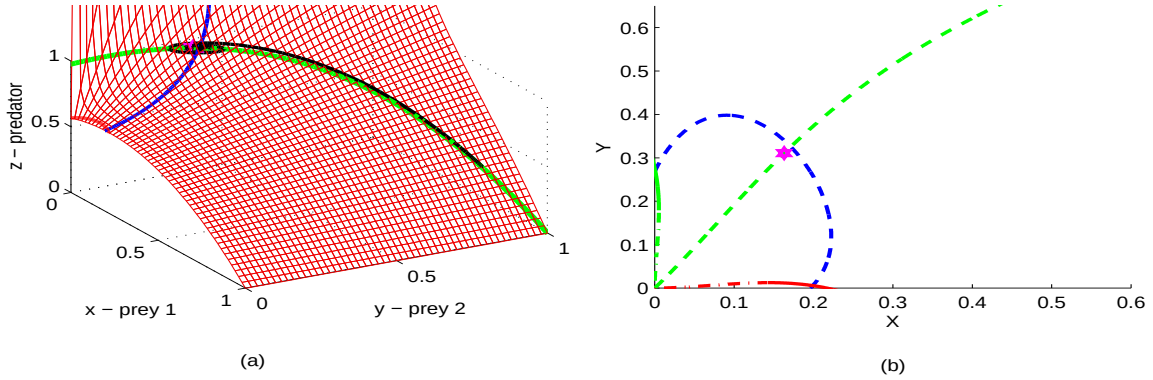

Figure 7: (a) A stable equilibrium point with parameter values: $\zeta = .001; \epsilon = .1; \delta = .257; \sigma = .41; \mu = .45; \nu = .282; \beta_1 = (1-\delta)/(1+\delta) - .0244; \beta_2 = (1-\delta\sigma/\nu)/(1+\delta\sigma/\nu) - .0065$, (b) x-fold, y-fold, xy-nullcline intersection, xy_{crash}, and z-nullcline projected in the xy-plane.

would persist with the addition of another prey if z were also efficient with respect to that prey. In fact, without the assumption that $T_1 = \frac{x}{x+cy}T$ and $T_2 = \frac{cy}{x+cy}T$, this equilibrium point in the three species food web is always unstable. However, a stable equilibrium point occurs in this model for the three-dimensional case. When the predator chooses how much time to spend on a prey depending on its density, the food web can be stabilized. A numerical simulation for this stable equilibrium case is shown in Fig.7(a). Fig.7(b) shows the folds and intersections for this case. There will not be a joint xy-crash. Surprisingly, the 'smart' predator in this model can stabilize the food web. The existence of a stable equilibrium point in the x-efficient, y-efficient case is a unique feature of this model.

6.4 Complex Behaviors

6.4.1 Shilnikov Orbit

If the parameter values are such that the equilibrium point is unstable, complex behaviors can occur for relaxed ϵ. A chaotic attractor known as a Shilnikov orbit [3] can occur. The numerical simulation for a Shilnikov orbit is seen in Fig.8(a). The intersection of the three nullclines occurs on the unstable portion of the xy-intersection line as seen in Fig.8(b). The orbit will pass through the outbreak fold and crash fold of the x-nullcline $f = 0$.

The formation of a Shilnikov attractor requires the equilibrium point, (x_*, y_*, z_*), to be an unstable spiral. A Shilnikov orbit is a homoclinic orbit, which spirals out from the equilibrium point, hits the outbreak fold, lands on the outbreak-crash portion of $f = 0$, hits the crash fold and then returns to the equilibrium point. The existence of such an orbit guarantees the existence of chaos [3].

Eq.2 is now analyzed for the parameters above by comparing the behavior to the nullcline analysis. In the fast subsystem, an orbit starting at a point (x_0, y_0, z_0) jumps to the point (x_1, y_0, z_0) on the x-nullcline surface. However, now that there is a larger value of ϵ, the solution will not follow the intermediate subsystem exactly. For the Shilnikov orbit, the orbit stays on the x-nullcline $f = 0$ and travels in the increasing z-direction until it crosses the crash fold on the x-nullcline $f = 0$. At that point, the population of x decreases rapidly until it reaches the stable portion of the x-nullcline. The orbit will then spiral around the unstable equilibrium point, (x_*, y_*, z_*), because ϵ is moderate. It will cross the outbreak fold on the x-nullcline $f = 0$, which will rapidly increase the x-population. The orbit will then proceed in a similar fashion as it did from the point (x_1, y_0, z_0).

To determine whether the behavior is really chaotic, the Lyapunov exponents are calculated. Lyapunov exponents measure the similarity of orbits for nearby initial

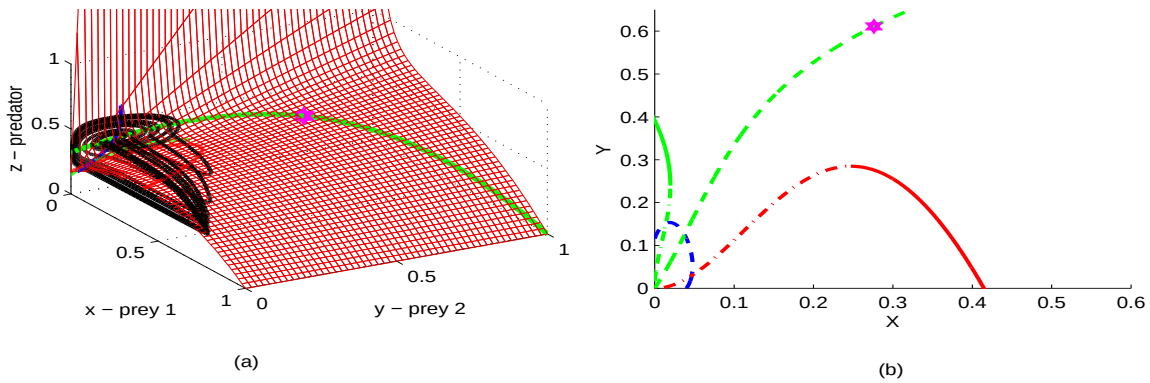

Figure 8: (a) A Shilnikov orbit with parameter values: $\zeta = .005; \epsilon = .612; \delta = .19; \sigma = .31; \mu = .45; \nu = .1689; \beta_1 = (1-\delta)/(1+\delta) - .51; \beta_2 = (1-\delta\sigma/\nu)/(1+\delta\sigma/\nu) - .2659$, (b) x-fold, y-fold, xy-nullcline intersection, xy_{crash}, and z-nullcline projected in the xy-plane.

conditions. Negative exponents imply that a small change in initial conditions does not have much effect. A positive Lyapunov exponent implies that a small change in initial conditions has a large effect. This is a characteristic of chaos. The Lyapunov exponents for this orbit were calculated using a Matlab program to be approximately .0728, $-.0006997$, and -21.4041. This small positive exponent, indicative of chaos, is significant especially since it would be larger for the original unscaled system as time-scaling the model also scales the Lyapunov exponents.

6.4.2 Two Cycle

Another possible behavior in the x-efficient, y-efficient case with moderate ϵ is a two cycle. This is seen in Fig.9(a). The projection of the folds and intersection lines is seen in Fig.9(b). In the two cycle, x and y crash at the joint xy-crash point as xy_{crash} occurs for $\dot{z} > 0$. The orbit then decreases in z and eventually an outbreak of x occurs. This is followed by a crash in x and an outbreak in x.

6.4.3 Rössler Attractor

For the x-efficient, y-efficient case, another possible long term dynamic for relaxed ϵ is a Rössler attractor. A numerical simulation showing a Rössler attractor is seen in Fig.10(a). The projection of the folds and intersection lines is seen in Fig.10(b). In this case, (x_*, y_*, z_*) is unstable as the xy-crash point occurs for $\dot{z} > 0$. Crashes and outbreaks in the population of x occur. The Lyapunov exponents for this Rössler attractor are .0281, $-.00030264$, and -15.6840. The small positive Lyapunov exponent

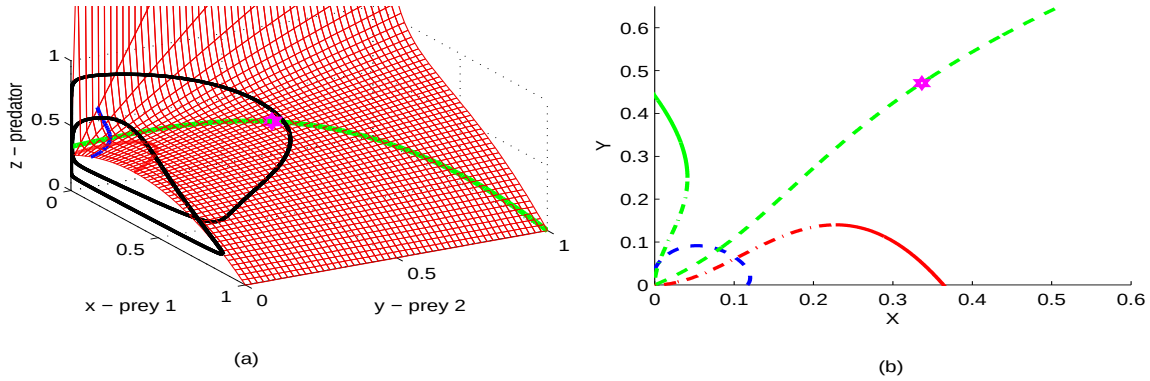

Figure 9: (a) A two cycle with parameter values: $\zeta = .1; \epsilon = .5; \delta = .3; \sigma = .31; \mu = .55; \nu = .393; \beta_1 = (1-\delta)/(1+\delta) - .2659; \beta_2 = (1-\delta\sigma/\nu)/(1+\delta\sigma/\nu) - .5$, (b) x-fold, y-fold, xy-nullcline intersection, xy_{crash}, and z-nullcline projected in the xy-plane.

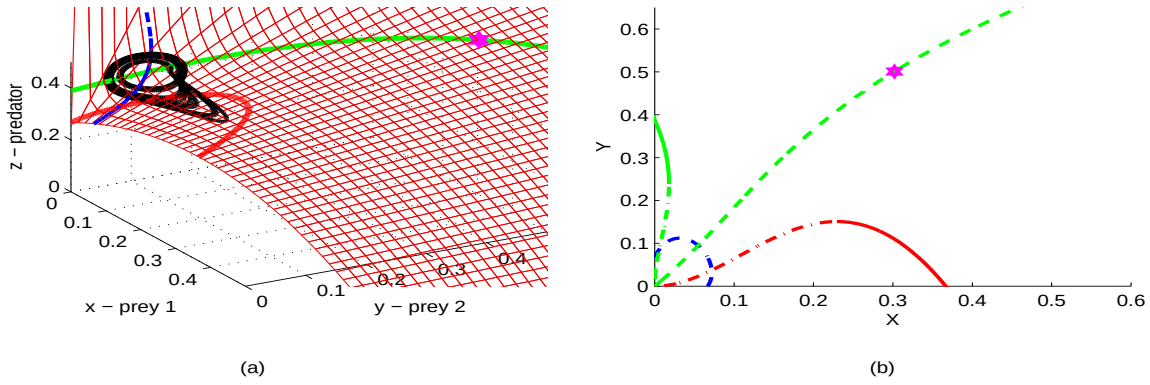

Figure 10: (a) A Rössler Attractor with parameter values: $\zeta = .01; \epsilon = 1; \delta = .2; \sigma = .3; \mu = .55; \nu = .26; \beta_1 = (1-\delta)/(1+\delta) - .4; \beta_2 = (1-\delta\sigma/\nu)/(1+\delta\sigma/\nu) - .4$, (b) x-fold, y-fold, xy-nullcline intersection, xy_{crash} and z-nullcline projected in the xy-plane.

shows that this is chaotic behavior.

7 Conclusion

When the predator divides its time between the two preys depending on the comparative density of the preys, this 'smart' predator has the ability to stabilize the food web. The x-efficient, y-efficient equilibrium point is possibly the most surprising behavior as a cycle occurs in the absence of either x or y. The occurrence of a joint xy-crash point stabilizes the food web when it occurs for $\dot{z} < 0$. When the joint xy-crash point occurs for $\dot{z} > 0$, the equilibrium is unstable. For the unstable equilibrium in the x-efficient, y-efficient case, different types of complex behavior can occur including limit cycles and chaotic behavior.

References

[1] Bockelman, B., E. Green, L. Lippitt, and J. Sherman, "Long Term Dynamics for Two Three-Species Food Webs," *Rose-Hulman Undergraduate Math Journal,* **4**(2), (2003).

[2] Deng, B., "Food chain chaos due to junction-fold point," *Chaos,* **11**(2001), pp.514-525.

[3] Deng, B., and G. Hines, "Food chain chaos due to Shilnikov's orbit," *Chaos,* **12**(2002), pp.533-538.

[4] Deng, B., and G. Hines, "Food chain chaos due to transcritical point," *Chaos,* **13**(2003), pp.575-585.

[5] Holling, C. S., "Some characteristics of simple types of predation and parasitism," *The Canadian Entomologist,* **91**(1959), pp.385-398.

[6] Liu, W., "Exchange Lemmas for Singularly Perturbed Problems with Certain Turning Points," *J. Diff. Eq.,* **167**(2000), pp.134-180.

[7] Mischenko, E.F., Yu. S. Kolesov, and N.Kh. Rozov, "Asymptotic Methods in Singularly Perturbed Equation," *Monographs in Contemporary Mathematics,* Consultants Bureau, New York, 1994.

[8] Schecter, S., "Persistent Unstable Equilibria and Closed Orbits of a Singularly Perturbed Equation," *J. Diff. Eq.,* **60**(1985), pp.131-141.